Available online at www.sciencedirect.com
SCIENCE DIRECT®
ELSEVIER
International Journal of Solids and Structures 43 (2006) 5628–5646
INTERNATIONAL JOURNAL OF SOLIDS and STRUCTURES
www.elsevier.com/locate/ijsolstr

Magneto–thermo–electro–elastic transient response in a piezoelectric hollow cylinder subjected to complex loadings

H.L. Dai [a,*], X. Wang [b]

[a] Department of Engineering and Mechanics, Hunan University, Changsha 410082, Hunan Province, PR China
[b] The School of Civil Engineering and Mechanics, Shanghai Jiao Tong University, Shanghai 200240, PR China

Received 5 May 2005; received in revised form 30 June 2005
Available online 8 September 2005

Abstract

The article presents an analytical solution for magneto–thermo–electro–elastic problems of a piezoelectric hollow cylinder placed in an axial magnetic field subjected to arbitrary thermal shock, mechanical load and transient electric excitation. Using an interpolation method solves the Volterra integral equation of the second kind caused by interaction among magnetic, thermal, electric and mechanical fields, the electric displacement is determined. Thus, the exact expressions for the transient responses of displacement, stresses, electric displacement, electric potential and perturbation of the magnetic field vector in the piezoelectric hollow cylinder are obtained by means of Hankel transforms, Laplace transforms, and inverse Laplace transforms. From sample numerical calculations, it is seen that the present method is suitable for a piezoelectric hollow cylinder subjected to arbitrary thermal shock, mechanical load and transient electric excitation, and the result carried out may be used as a reference to solve other transient coupled problems of magneto–thermo–electro–elasticity.

Keywords: Magneto–thermo–electro–elastic; Piezoelectric hollow cylinder; Transient; Perturbation of magnetic field vector

1. Introduction

Increased interest in magneto–thermo–electro–elasticity during recent years can be attributed to the fact that the study of magneto–thermo–electro–mechanical coupled behavior in smart structures. The interaction among magnetic, thermal, electric and mechanical fields in a piezoelectric hollow cylinder is usually encountered in space shuttles, supersonic airplanes, rockets and missiles, plasma physics and the

* Corresponding author. Tel./fax: +86 07318822330.
E-mail address: hldai520@sina.com (H.L. Dai).

0020-7683/$ - see front matter © 2005 Published by Elsevier Ltd.
doi:10.1016/j.ijsolstr.2005.06.092

Nomenclature

u_r, $\vec{U}$	radial displacement [m] and displacement vector
c_{ij}, e_{ij}	elastic constants [N/m^2] and piezoelectric constants [C/m^2]
g_{11}, β_1	dielectric constants [C^2/N m^2] and pyroelectric constants [C/m^2 K]
α_i, λ_i	thermal constants [1/K] and thermal modulus [N/m^2 K]
σ_{ii}, D_{rr}	the component of stresses [N/m^2] and radial electric displacement [C/m^2]
$\varphi(r,t)$	electric potential [V]
$T(r,t)$	temperature change [K]
ρ, t	mass density [kg/m^3] and time [s]
$\vec{H}$, $\vec{h}$	magnetic intensity vector and perturbation of magnetic field vector
J	electric current density vector
$\vec{e}$	perturbation of electric field vector
μ	magnetic permeability [H/m]
f_{zz}	Lorentz's force [kg/m^2 s^2]
r, θ, z	radial variable, circumferential variable and axial variable [m]
a, b	inner and outer radii of piezoelectric hollow cylinder [m]
$P_{a0}(t)$, $P_{b0}(t)$	internal and external pressure of piezoelectric hollow cylinder [kg/m^2 s^2]
$\varphi_a(t)$, $\varphi_b(t)$	internal and external electric potential of piezoelectric hollow cylinder [V]
u_{r0}, v_{r0}	initial radial displacement [m] and initial speed [m/s]
C_L	electromagnetothermoelastic wave speed [m/s]
ω	the inherent frequency of the piezoelectric hollow cylinder [1/s]

corresponding measurement techniques of magneto–thermo–electro–elasticity. The interaction among magnetic, thermal, electric and mechanical fields in a piezoelectric hollow cylinder gives rise to the transient coupled theory of magneto–thermo–electro–elasticity. The theory is applicable to analyze a wide range of magnetically, thermally, electrically and mechanically coupled phenomena in the mixed state.

Shul'ga et al. (1984) investigated the axisymmetric electroelastic waves in a piezoelectric hollow ceramic cylinder. An exact solution for the static analysis of a simply-supported piezoelectric plate and a layered intelligent plate under cylindrical bending was presented by Ray et al. (1992, 1993). Mithchell and Reddy (1995) presented a power series solution for the static analysis of an axisymmetric composite cylinder with surface bonded or embedded piezoelectric laminate. Chandrasekhararaiah (1988) gave a generalized linear theory for piezoelectric media. A classical laminated plate theory was used by Tauchert (1992) to investigate the response of a thin composite plate coupled with piezothermoelastic layers, subjected to combined thermal and electrical excitations. Finite element formulations for piezothermoelastic materials to demonstrate their ability for distributed sensing and distributed precision control of advanced intelligent structures were given by Rao and Sunar (1993, 1994). Exact piezothermoelastic solutions of a finite transversely isotropic piezoelectric cylindrical shell under axisymmetric thermal, pressure and electrostatic excitation and a simply-supported hybrid cylindrical shell made of cross-ply composite laminate and piezoelectric layers were presented by Kapuria et al. (1996, 1997). The free vibrations of piezoelectric, empty and also compressible fluid filled cylindrical shells for three-dimensional problems were studied by Ding et al. (1997). By means of using the linear equations of piezothermoelasticity, Raja et al. (1999) presented a generalized piezothermoelastic finite element formulation of a laminated beam with embedded piezoelectric material as distributed actuators/sensors. Wang and Lu (2002) presented a theoretical method to analyze magneto–thermo–elastic waves and perturbation of the magnetic field vector produced by thermal shock in a solid conducting

cylinder. By virtue of the separation of variables technique, the axisymmetric plane strain electroelastic dynamic problem of hollow cylinder was investigated by Ding et al. (2003). Dai and Wang (2004) presented an analytical solution for the interaction of electric potential, electric displacement, elastic deformations and mechanical loads, and described electromagnetoelastic responses and perturbation of the magnetic field vector in a piezoelectric hollow cylinder subjected to sudden mechanical load and electric potential.

To date investigations on the interaction of thermo–electro–mechanical coupled behavior in piezoelectric structures have mainly considered a transient interaction among thermal, electric and mechanical fields, and transient electric interaction between electric field and mechanical field. However, investigations on magneto–thermo–electro–elastic transient response of a piezoelectric structure placed in an axial magnetic field subjected to arbitrary thermal shock, mechanical load and transient electric excitation have been very few.

In this paper, the magneto–thermo–electro–elastic equation of a piezoelectric hollow cylinder is decomposed into a quasi-static homogeneous equation with inhomogeneous boundary conditions and an inhomogeneous dynamic equation with homogeneous boundary conditions. Firstly, using the method described by Lekhniskii (1981), the quasi-static question is solved by the direct integral. Secondly, the solution to the inhomogeneous dynamic question which satisfies homogeneous boundary conditions is obtained by utilizing the corresponding finite Hankel transforms (Cinelli, 1965), the Laplace transforms and their inverse transforms. Then, using an interpolation method solves the Volterra integral equation of the second kind caused by interaction among magnetic, thermal, electric and mechanical fields. Thus, the exact expressions for the transient responses of displacements, stresses, electric displacement, electric potential and perturbation of magnetic field vector in the piezoelectric hollow cylinder are obtained. Finally, numerical examples are calculated and discussed.

2. Basic formulations

Considering a long, piezoelectric hollow cylinder with internal radius a and external radius b in an axial magnetic field $H(0,0,H_z)$, letting the cylindrical coordinates of any representative point be (r,θ,z), and assuming that the piezoelectric hollow cylinder is subjected to a rapid change in temperature $T(r,t)$. For the axisymetric plane strain problem, the components of displacement and electric potential in the cylindrical coordinate (r,θ,z) system are expressed as $u_0 = u_z = 0$, $u_r = u_r(r,t)$ and $\varphi = \varphi(r,t)$, respectively. The constitutive relations of piezoelectric media are expressed as

$$\sigma_{rr} = c_{11}\frac{\partial u_r}{\partial r} + c_{12}\frac{u_r}{r} + e_{11}\frac{\partial \varphi}{\partial r} - \lambda_1 T(r,t), \tag{1a}$$

$$\sigma_{\theta\theta} = c_{12}\frac{\partial u_r}{\partial r} + c_{22}\frac{u_r}{r} + e_{12}\frac{\partial \varphi}{\partial r} - \lambda_2 T(r,t), \tag{1b}$$

$$\sigma_{zz} = c_{13}\frac{\partial u_r}{\partial r} + c_{23}\frac{u_r}{r} + e_{13}\frac{\partial \varphi}{\partial r} - \lambda_3 T(r,t), \tag{1c}$$

$$D_{rr} = e_{11}\frac{\partial u_r}{\partial r} + e_{12}\frac{u_r}{r} - g_{11}\frac{\partial \varphi}{\partial r} + \beta_1 T(r,t), \tag{1d}$$

$$\lambda_1 = c_{11}\alpha_1 + c_{12}\alpha_2 + c_{13}\alpha_3, \quad \lambda_2 = c_{12}\alpha_1 + c_{22}\alpha_2 + c_{23}\alpha_3, \quad \lambda_3 = c_{13}\alpha_1 + c_{23}\alpha_2 + c_{33}\alpha_3, \tag{1e}$$

where c_{ij}, e_{ij}, α_i, g_{11} and β_1 are elastic constants, piezoelectric constants, thermal expansion coefficients, dielectric constants, and pyroelectric coefficients, respectively. σ_{ii} and D_{rr} are the component of stresses and radial electric displacement, respectively.

The boundary conditions are

$$\sigma_{rr}(a,t) = P_{a0}(t), \quad \sigma_{rr}(b,t) = P_{b0}(t), \quad \varphi(a,t) = \varphi_a(t), \quad \varphi(b,t) = \varphi_b(t). \tag{2}$$

The initial conditions are

$$[u_r(r,t)]_{t=0} = u_{r0}(r), \quad \left[\frac{\partial u_r(r,t)}{\partial t}\right]_{t=0} = v_{r0}(r). \tag{3}$$

Assuming that the magnetic permeability, μ, of the piezoelectric hollow cylinder equals the magnetic permeability of the medium around it, the governing electrodynamic Maxwell equations (Kraus, 1984) are given by

$$\bar{J} = \nabla \times \bar{h}, \quad \nabla \times \bar{e} = -\mu \frac{\partial \bar{h}}{\partial t}, \quad \text{div}\, \bar{h} = 0, \quad \bar{e} = -\mu\left(\frac{\partial \bar{U}}{\partial t} \times \bar{H}\right), \quad \bar{h} = \nabla \times (\bar{U} \times \bar{H}). \tag{4}$$

Applying an initial magnetic field vector $\bar{H}(0,0,H_z)$ in the hollow cylindrical coordinate (r,θ,z) to Eq. (4), yields

$$\begin{aligned} &\bar{U} = (u_r, 0, 0), \quad \bar{e} = -\mu\left(0, H_z \frac{\partial u_r}{\partial t}, 0\right), \quad \bar{h} = (0,0,h_z), \\ &\bar{J} = \left(0, -\frac{\partial h_z}{\partial r}, 0\right), \quad h_z = -H_z\left(\frac{\partial u_r}{\partial r} + \frac{u_r}{r}\right). \end{aligned} \tag{5}$$

The electomagnetic dynamic equation of the piezoelectric hollow cylinder is expressed as

$$\frac{\partial \sigma_{rr}}{\partial r} + \frac{\sigma_{rr} - \sigma_{\theta\theta}}{r} + f_{zz} = \rho \frac{\partial^2 u_r}{\partial t^2}, \tag{6}$$

where ρ is the mass density, f_{zz} is defined as Lorentz's force (Kraus, 1984), which may be written as

$$f_{zz} = \mu(\bar{J} \times \bar{H}) = \mu H_z^2 \frac{\partial}{\partial r}\left(\frac{\partial u_r}{\partial r} + \frac{u_r}{r}\right). \tag{7}$$

In order to simplify calculation, the non-dimensional forms are introduced as follows:

$$\begin{aligned} &c_1 = \frac{c_{12}}{c_{11}}, \quad c_2 = \frac{c_{22}}{c_{11}}, \quad c_3 = \frac{c_{13}}{c_{11}}, \quad c_4 = \frac{c_{23}}{c_{11}}, \quad e_i = \frac{e_{1i}}{\sqrt{c_{11}g_{11}}} \quad (i = 1,2,3), \\ &\sigma_i = \frac{\sigma_{ii}}{c_{11}} \quad (i = r,\theta), \quad \phi = \sqrt{\frac{g_{11}}{c_{11}}}\frac{\varphi}{b}, \quad D_r = \frac{D_{rr}}{\sqrt{c_{11}g_{11}}}, \quad T_i(\xi,\tau) = \frac{\lambda_i T(r,t)}{c_{11}} \quad (i = 1,2,3), \\ &T_\beta(\xi,\tau) = \frac{\beta_1 T(r,t)}{\sqrt{c_{11}g_{11}}}, \quad u = \frac{u_r}{b}, \quad \xi = \frac{r}{b}, \quad s = \frac{a}{b}, \quad C_V = \sqrt{\frac{c_{11}}{\rho}}, \quad \tau = \frac{C_V t}{b}, \quad f_z = \frac{f_{zz}}{c_{11}}b, \\ &P_a(\tau) = \frac{P_{a0}(t)}{c_{11}}, \quad P_b(\tau) = \frac{P_{b0}(t)}{c_{11}}, \quad \phi_a(\tau) = \sqrt{\frac{g_{11}}{c_{11}}}\frac{\varphi(a,t)}{b}, \quad \phi_b(\tau) = \sqrt{\frac{g_{11}}{c_{11}}}\frac{\varphi(b,t)}{b} \end{aligned} \tag{8}$$

then, Eqs. (1), (6) and (7) can be rewritten as

$$\sigma_r = \frac{\partial u}{\partial \xi} + c_1\frac{u}{\xi} + e_1\frac{\partial \phi}{\partial \xi} - T_1(\xi,\tau), \tag{9a}$$

$$\sigma_\theta = c_1\frac{\partial u}{\partial \xi} + c_2\frac{u}{\xi} + e_2\frac{\partial \phi}{\partial \xi} - T_2(\xi,\tau), \tag{9b}$$

$$\sigma_z = c_3\frac{\partial u}{\partial \xi} + c_4\frac{u}{\xi} + e_3\frac{\partial \phi}{\partial \xi} - T_3(\xi,\tau), \tag{9c}$$

$$D_r = e_1\frac{\partial u}{\partial \xi} + e_2\frac{u}{\xi} - \frac{\partial \phi}{\partial \xi} + T_\beta(\xi,\tau), \tag{9d}$$

$$\frac{\partial \sigma_r}{\partial \xi} + \frac{\sigma_r - \sigma_\theta}{\xi} = \frac{\partial^2 u}{\partial \tau^2}, \tag{9e}$$

$$f_z = \frac{\mu H_z^2}{c_{11}}\frac{\partial}{\partial \xi}\left(\frac{\partial u}{\partial \xi} + \frac{u}{\xi}\right). \tag{9f}$$

In absence of free charge density, the charge equation of electrostatics is

$$\frac{\partial D_r(\xi,\tau)}{\partial \xi}+\frac{D_r}{\xi}=0. \tag{10}$$

From Eq. (10), gives

$$D_r(\xi,\tau)=\frac{1}{\xi}d(\tau), \tag{11}$$

where $d(\tau)$ is an undetermined function to non-dimensional time τ.

According to Eq. (8), the boundary conditions (2) and the initial conditions (3) are rewritten as

$$\sigma_r(s,\tau)=P_a(\tau),\quad \sigma_r(1,\tau)=P_b(\tau),\quad \phi(s,\tau)=\phi_a(\tau),\quad \phi(1,\tau)=\phi_b(\tau), \tag{12a}$$

$$[u(\xi,\tau)]_{\tau=0}=u_0(\xi),\quad \left[\frac{\partial u(\xi,\tau)}{\partial \tau}\right]_{\tau=0}=v_0(\xi). \tag{12b}$$

Substituting Eq. (11) into Eq. (9d), gives

$$\frac{\partial \phi}{\partial \xi}=e_1\frac{\partial u}{\partial \xi}+e_2\frac{u}{\xi}-\frac{1}{\xi}d(\tau)+T_\beta(\xi,\tau). \tag{13}$$

Substituting Eq. (13) into Eqs. (9a) and (9b), yields,

$$\sigma_r=(1+e_1^2)\frac{\partial u}{\partial \xi}+(c_1+e_1e_2)\frac{u}{\xi}-\frac{e_1}{\xi}d(\tau)-T_{1\beta}(\xi,\tau), \tag{14a}$$

$$\sigma_\theta=(c_1+e_1e_2)\frac{\partial u}{\partial \xi}+(c_2+e_2^2)\frac{u}{\xi}-\frac{e_2}{\xi}d(\tau)-T_{2\beta}(\xi,\tau), \tag{14b}$$

where

$$T_{1\beta}(\xi,\tau)=T_1(\xi,\tau)-e_1T_\beta(\xi,\tau),T_{2\beta}(\xi,\tau)=T_2(\xi,\tau)-e_2T_\beta(\xi,\tau). \tag{14c}$$

Substituting Eq. (14a,b) into Eq. (9e), the basic displacement equation of magneto–thermo–electro–elastic motion of the piezoelectric hollow cylinder is expressed as

$$\frac{\partial^2 u(\xi,\tau)}{\partial \xi^2}+\frac{1}{\xi}\frac{\partial u(\xi,\tau)}{\partial \xi}-\frac{H^2u(\xi,\tau)}{\xi^2}=\frac{1}{C_L^2}\frac{\partial^2 u(\xi,\tau)}{\partial \tau^2}+I\frac{d(\tau)}{\xi^2}+g(\xi,\tau), \tag{15a}$$

where

$$H=\sqrt{\frac{c_{11}(c_2+e_2^2)+\mu H_z^2}{c_{11}(1+e_1^2)+\mu H_z^2}},\quad C_L=\sqrt{\frac{c_{11}(1+e_1^2)+\mu H_z^2}{c_{11}}},$$

$$I=-\frac{c_{11}e_2}{c_{11}(1+e_1^2)+\mu H_z^2},\quad g(\xi,\tau)=\frac{1}{c_{11}(1+e_1^2)+\mu H_z^2}\left[\frac{\partial T_{1\beta}}{\partial \xi}+\frac{1}{\xi}(T_{1\beta}-T_{2\beta})\right]. \tag{15b}$$

Substituting Eq. (14a) into Eq. (12a), the corresponding stress boundary conditions are rewritten as

$$\left[\frac{\partial u(\xi,\tau)}{\partial \xi}+h\frac{u(\xi,\tau)}{\xi}\right]_{\xi=s}=\theta_1(\tau), \tag{16a}$$

$$\left[\frac{\partial u(\xi,\tau)}{\partial \xi}+h\frac{u(\xi,\tau)}{\xi}\right]_{\xi=1}=\theta_2(\tau), \tag{16b}$$

where

$$h=\frac{c_1+e_1e_2}{1+e_1^2},\quad \theta_1(\tau)=\frac{1}{1+e_1^2}\left[\frac{e_1}{s}d(\tau)+T_{1\beta}(s,\tau)+p_a(\tau)\right],$$
$$\theta_2(\tau)=\frac{1}{1+e_1^2}\left[e_1d(\tau)+T_{1\beta}(1,\tau)+p_b(\tau)\right]. \tag{16c}$$

3. Solving technique

Assuming that the general solution to the basic displacement Eq. (15) of magneto–thermo–electro–elastic motion is expressed in the form

$$u(\xi,\tau)=u_{\mathrm{q}}(\xi,\tau)+u_{\mathrm{d}}(\xi,\tau), \tag{17}$$

where $u_{\mathrm{q}}(\xi,\tau)$ and $u_{\mathrm{d}}(\xi,\tau)$ are, respectively, the quasi-static solution which satisfies inhomogeneous boundary conditions and dynamic solution which satisfies homogeneous boundary conditions, to Eq. (15a).

The quasi-static solution $u_{\mathrm{q}}(\xi,\tau)$ must satisfy the following Eq. (18a) and the corresponding inhomogeneous boundary conditions Eq. (18b–c).

$$\frac{\partial^2u_{\mathrm{q}}(\xi,\tau)}{\partial\xi^2}+\frac{1}{\xi}\frac{\partial u_{\mathrm{q}}(\xi,\tau)}{\partial\xi}-\frac{H^2}{\xi^2}u_{\mathrm{q}}(\xi,\tau)=I\frac{d(\tau)}{\xi^2}+g(\xi,\tau), \tag{18a}$$
$$\left[\frac{\partial u_{\mathrm{q}}(\xi,\tau)}{\partial\xi}+h\frac{u_{\mathrm{q}}(\xi,\tau)}{\xi}\right]_{\xi=s}=\theta_1(\tau), \tag{18b}$$
$$\left[\frac{\partial u_{\mathrm{q}}(\xi,\tau)}{\partial\xi}+h\frac{u_{\mathrm{q}}(\xi,\tau)}{\xi}\right]_{\xi=1}=\theta_2(\tau). \tag{18c}$$

Eq. (18a) can simplify to

$$\frac{\partial}{\partial\xi}\left[\xi^{-(2H-1)}\frac{\partial}{\partial\xi}(\xi^Hu_{\mathrm{q}}(\xi,\tau))\right]=\xi^{-H+1}[I\xi^{-2}d(\tau)+g(\xi,\tau)]. \tag{19}$$

From Eq. (19) the quasi-static solution for Eq. (18a), which satisfies the boundary condition Eq. (18b–c) is expressed as

$$u_{\mathrm{q}}(\xi,\tau)=\psi_1(\xi,\tau)+\psi_2(\xi)p_a(\tau)+\psi_3(\xi)p_b(\tau)+\psi_4(\xi)d(\tau), \tag{20}$$

where

$$\psi_1(\xi,\tau)=\xi^{-H}\int_s^\xi\xi^{2H-1}\int_s^\xi\xi^{-H+1}g(\xi,\tau)\,\mathrm{d}\xi\,\mathrm{d}\xi + \left[\frac{\xi^{2H}-s^{2H}}{2H}-\frac{s^{2H}}{h-H}\right]\xi^{-H}q_3(\tau)+\frac{s^{H+1}T_{1\beta}(s,\tau)}{(h-H)C_L^2}\xi^{-H}, \tag{21a}$$
$$\psi_2(\xi)=\frac{s^{H+1}\xi^{-H}}{C_L^2}\left[-\frac{g_2(\xi^{2H}-s^{2H})}{2H}+\frac{g_2s^{2H}+1}{(h-H)}\right] \tag{21b}$$
$$\psi_3(\xi)=\frac{g_2\xi^{-H}}{C_L^2}\left[\frac{(\xi^{2H}-s^{2H})}{2H}-\frac{s^{2H}}{(h-H)}\right], \tag{21c}$$
$$\psi_4(\xi)=I\frac{s^H\xi^{-H}-2+s^{-H}\xi^H}{2H^2}, + g_3\left[\frac{\xi^{2H}-s^{2H}}{2H}-\frac{s^{2H}}{h-H}\right]\xi^{-H}+\frac{e_1s^H}{(h-H)C_L^2}\xi^{-H}, \tag{21d}$$

$$g_3 = g_2\left[(H-h)g_1 + \frac{I(1-s^{-H})}{H} + \frac{e_1}{C_L^2}(1-s^H)\right],$$
$$g_2 = \frac{2H}{(1-s^{2H})(H+h)}, \quad g_1 = \frac{-2+s^{-H}+s^H}{2H},$$
$$q_1(\tau) = \int_s^1 \xi^{2H-1}\int_s^\xi \xi^{-H+1}g(\xi,\tau)\,\mathrm{d}\xi\,\mathrm{d}\xi, \quad q_2(\tau) = \int_s^1 \xi^{-H+1}g(\xi,\tau)\,\mathrm{d}\xi,$$
$$q_3(\tau) = g_2\left\{(H-h)q_1(\tau) - q_2(\tau) + \frac{1}{C_L^2}[T_{1\beta}(1,\tau) - s^{H+1}T_{1\beta}(s,\tau)]\right\}, \tag{21e–j}$$

Substituting Eq. (17) into Eq. (15a) and utilizing Eq. (16a,b) and Eq. (18) provides an inhomogeneous dynamic equation with homogeneous boundary conditions, and the corresponding initial conditions for $u_{\mathrm{d}}(\xi,\tau)$

$$\frac{\partial^2 u_{\mathrm{d}}(\xi,\tau)}{\partial\xi^2} + \frac{1}{\xi}\frac{\partial u_{\mathrm{d}}(\xi,\tau)}{\partial\xi} - \frac{H^2}{\xi^2}u_{\mathrm{d}}(\xi,\tau) = \frac{1}{C_L^2}\left[\frac{\partial^2 u_{\mathrm{d}}(\xi,\tau)}{\partial\tau^2} + \frac{\partial^2 u_{\mathrm{q}}(\xi,\tau)}{\partial\tau^2}\right], \tag{22a}$$
$$\left[\frac{\partial u_{\mathrm{d}}(\xi,\tau)}{\partial\xi} + h\frac{u_{\mathrm{d}}(\xi,\tau)}{\xi}\right]_{\xi=s} = 0, \left[\frac{\partial u_{\mathrm{d}}(\xi,\tau)}{\partial\xi} + h\frac{u_{\mathrm{d}}(\xi,\tau)}{\xi}\right]_{\xi=1} = 0, \tag{22b}$$
$$u_{\mathrm{d}}(\xi,0) + u_{\mathrm{q}}(\xi,0) = u_0, \quad \frac{\partial u_{\mathrm{d}}(\xi,0)}{\partial\tau} + \frac{\partial u_{\mathrm{q}}(\xi,0)}{\partial\tau} = v_0. \tag{22c}$$

In the above equation, $u_{\mathrm{q}}(\xi,\tau)$ is the known solution as shown in Eq. (20).

The homogeneous equation (let $u_{\mathrm{q}}(\xi,\tau) = 0$) of Eq. (22a) with homogeneous boundary (22b) is solved by assuming

$$u_{\mathrm{d}}(\xi,\tau) = u_{\mathrm{d}i}(\xi)\exp(\mathrm{i}\omega\tau). \tag{23}$$

The corresponding Eigen-equation is expressed as

$$J_a Y_b - J_b Y_a = 0, \tag{24}$$

where

$$J_a = k_i J'_H(k_i s) + h\frac{J_H(k_i s)}{s}, \quad J_b = k_i J'_H(k_i) + hJ_H(k_i), \tag{25a}$$
$$Y_a = k_i Y'_H(k_i s) + h\frac{Y_H(k_i s)}{s}, \quad Y_b = k_i Y'_H(k_i) + hY_H(k_i). \tag{25b}$$

$J_H(k_i\xi)$and $Y_H(k_i\xi)$ are the first and the second kind of the Hth-order Bessel function, respectively. In these expressions, $k_i\,(i = 1, 2, \ldots, n)$ express a series of positive roots for natural Eigen-equation (24). The natural frequencies are

$$\omega_i = C_L k_i. \tag{26}$$

From Cinelli (1965), defining $\bar{u}_{\mathrm{d}}(k_i,\tau)$as the finite Hankel transform of the solution $u_{\mathrm{d}}(\xi,\tau)$ for Eq. (22a), yields

$$\bar{u}_{\mathrm{d}}(k_i,\tau) = H[u_{\mathrm{d}}(\xi,\tau)] = \int_s^1 \xi u_{\mathrm{d}}(\xi,\tau)G_H(k_i\xi)\,\mathrm{d}\xi. \tag{27}$$

Then, by making use of the inverse of the transform, yields

$$u_{\mathrm{d}}(\xi,\tau) = \sum_{k_i}\frac{\bar{u}_{\mathrm{d}}(k_i,\tau)}{F(k_i)}G_H(k_i\xi), \tag{28}$$

where

$$F(k_i) = \int_s^1 \xi[G_H(k_i\xi)]^2 \,\mathrm{d}\xi,$$
$$= \frac{J_a^2}{J_b^2}\frac{2}{k_i^2\pi^2}\left\{h^2 + k_i^2\left[1 - \left(\frac{H}{k_i}\right)^2\right]\right\} - \frac{2}{k_i^2\pi^2}\left\{\left(\frac{h}{s}\right)^2 + k_i^2\left[1 - \left(\frac{H}{k_i s}\right)^2\right]\right\}, \tag{29a}$$
$$G_H(k_i\xi) = J_H(k_i\xi)Y_a - J_a Y_H(k_i\xi). \tag{29b}$$

Applying the finite Hankel transform (27) to Eq. (22a) and utilizing the corresponding boundary condition (22b), gives

$$-k_i^2\bar{u}_\mathrm{d}(k_i,\tau) = \frac{1}{C_L^2}\left[\frac{\partial^2\bar{u}_\mathrm{d}(k_i,\tau)}{\partial\tau^2} + \frac{\partial^2\bar{u}_\mathrm{q}(k_i,\tau)}{\partial\tau^2}\right], \tag{30}$$

where $\bar{u}_\mathrm{q}(k_i,\tau) = H[u_\mathrm{q}(\xi,\tau)]$.

Applying the Laplace transform to the two sides of Eq. (30) and utilizing the initial condition (22c), yields

$$-k_i^2 C_L^2\bar{u}_\mathrm{d}^*(k_i,p) = p^2\bar{u}_\mathrm{d}^*(k_i,p) + p^2\bar{u}_\mathrm{q}^*(k_i,p) - p\bar{u}_0(k_i) - \bar{v}_0(k_i), \tag{31}$$

where p is the parameter of the Laplace transform.

Eq. (31) can be simplified to

$$\bar{u}_\mathrm{d}^*(k_i,p) = -\bar{u}_\mathrm{q}^*(k_i,p) + \frac{\omega_i^2}{(\omega_i^2+p^2)}\bar{u}_\mathrm{q}^*(k_i,p) + \frac{p\bar{u}_0(k_i)}{(\omega_i^2+p^2)} + \frac{\bar{v}_0(k_i)}{(\omega_i^2+p^2)}, \tag{32}$$

where $\bar{u}_0(k_i) = H[u_0(\xi)]$ and $\bar{v}_0(k_i) = H[v_0(\xi)]$.

The inverse Laplace transform for Eq. (32), gives

$$\bar{u}_\mathrm{d}(k_i,\tau) = -\bar{u}_\mathrm{q}(k_i,\tau) + \omega_i[\bar{u}_\mathrm{q}(k_i,\tau)\sin(\omega_i\tau)] + \bar{u}_0(k_i)\cos(\omega_i\tau) + \frac{\bar{v}_0(k_i)}{\omega_i}\sin(\omega_i\tau), \tag{33}$$

where

$$\bar{u}_\mathrm{q}(k_i,\tau)\sin(\omega_i\tau) = \int_0^\tau \bar{u}_\mathrm{q}(k_i,t)\sin[\omega_i(\tau-t)]\,\mathrm{d}t. \tag{34}$$

Substituting Eq. (34) into Eq. (33), gives

$$\bar{u}_\mathrm{q}(k_i,\tau)\sin(\omega_i\tau) = \int_0^\tau [\bar{\psi}_1(k_i,\tau) + \bar{\psi}_2(k_i)p_a(\tau) + \bar{\psi}_3(k_i)p_b(\tau) + \bar{\psi}_4(k_i)d(\tau)]\sin[\omega_i(\tau-t)]\,\mathrm{d}t, \tag{35}$$

where $\bar{\psi}_j(k_i,\tau) = H[\psi_j(\xi,\tau)]$, $(j = 1,2,3,4)$.

Substituting Eq. (35) into Eq. (33), yields

$$\bar{u}_\mathrm{d}(k_i,\tau) = I_{1i}(k_i,\tau) + \bar{\psi}_2(k_i)I_{2i}(k_i,\tau) + \bar{\psi}_3(k_i)I_{3i}(k_i,\tau) + \bar{\psi}_4(k_i)I_{4i}(k_i,\tau) + I_{5i}(k_i,\tau), \tag{36}$$

where

$$
\begin{aligned}
I_{1i}(k_i,\tau) &= -\bar{\psi}_1(k_i,\tau) + \omega_i \int_0^\tau \bar{\psi}_1(k_i,t)\sin[\omega_i(\tau-t)]\,\mathrm{d}t,\\
I_{2i}(k_i,\tau) &= -p_a(\tau) + \omega_i \int_0^\tau p_a(t)\sin[\omega_i(\tau-t)]\,\mathrm{d}t,\\
I_{3i}(k_i,\tau) &= -p_b(\tau) + \omega_i \int_0^\tau p_b(\tau)\sin[\omega_i(\tau-t)]\,\mathrm{d}t,\\
I_{4i}(k_i,\tau) &= -d(\tau) + \omega_i \int_0^\tau d(t)\sin[\omega_i(\tau-t)]\,\mathrm{d}t,\\
I_{5i}(k_i,\tau) &= \bar{u}_0(k_i)\cos(\omega_i\tau) + \bar{v_0}(k_i)\frac{1}{\omega_i}\sin(\omega_i\tau).
\end{aligned}
\tag{37}
$$

Substituting Eq. (36) into Eq. (28), the dynamic solution for inhomogeneous dynamic equation (22) with homogeneous boundary conditions is given by

$$
u_{\mathrm{d}}(\xi,\tau) = \sum_{k_i}\frac{G_H(k_i\xi)}{F(k_i)}[I_{1i}(k_i,\tau) + \bar{\psi}_2(k_i)I_{2i}(k_i,\tau) + \bar{\psi}_3(k_i)I_{3i}(k_i,\tau) + \bar{\psi}_4(k_i)I_{4i}(k_i,\tau) + I_{5i}(k_i,\tau)]. \tag{38}
$$

Thus, from Eqs. (17), (20) and (38), the solution of the basic displacement equation of magneto–thermo–electro–elastic motion in the piezoelectric hollow cylinder is expressed as

$$
\begin{aligned}
u(\xi,\tau) = {} & \psi_1(\xi,\tau) + \psi_2(\xi)p_a(\tau) + \psi_3(\xi)p_b(\tau) + \psi_4(\xi)d(\tau) + \sum_{k_i}\frac{G_H(k_i\xi)}{F(k_i)}\\
& \times [I_{1i}(k_i,\tau) + \bar{\psi}_2(k_i)I_{2i}(k_i,\tau) + \bar{\psi}_3(k_i)I_{3i}(k_i,\tau) + \bar{\psi}_4(k_i)I_{4i}(k_i,\tau) + I_{5i}(k_i,\tau)].
\end{aligned}
\tag{39}
$$

Noting that in the above expression $d(\tau)$ still is an unknown function which is relation to the electric displacement. Thus, it is necessary to determine $d(\tau)$ in the following.

Integrating Eq. (13) and utilizing the corresponding electric boundary condition (12a), yields

$$
\phi(\xi,\tau) = \Phi_1(\xi,\tau) + \Phi_2(\xi)p_a(\tau) + \Phi_3(\xi)p_b(\tau) + \Phi_4(\xi)d(\tau) + \sum_i \Phi_{5i}(\xi)F_i(\tau) + \phi_a(\tau), \tag{40}
$$

where

$$
\begin{aligned}
\Phi_1(\xi,\tau) = {} & e_1\left[\psi_1(\xi,\tau) - \psi_1(s,\tau) - \sum_{k_i}\frac{(G_H(k_i\xi) - G_H(k_is))}{F(k_i)}\bar{\psi}_1(k_i,\tau)\right]\\
& + e_2\int_s^\xi \frac{1}{\xi}\left[\psi_1(\xi,\tau) - \sum_{k_i}\frac{G_H(k_i\xi)}{F(k_i)}\bar{\psi}_1(k_i,\tau)\right]\mathrm{d}\xi + \int_s^\xi T_\beta(\xi,\tau)\,\mathrm{d}\xi,
\end{aligned}
\tag{41a}
$$

$$
\begin{aligned}
\Phi_2(\xi) = {} & e_1\left[\psi_2(\xi) - \psi_2(s) - \sum_{k_i}\frac{(G_H(k_i\xi) - G_H(k_is))}{F(k_i)}\bar{\psi}_2(k_i)\right]\\
& + e_2\int_s^\xi \frac{1}{\xi}\left[\psi_2(\xi) - \sum_{k_i}\frac{G_H(k_i\xi)}{F(k_i)}\bar{\psi}_2(k_i)\right]\mathrm{d}\xi,
\end{aligned}
\tag{41b}
$$

$$
\begin{aligned}
\Phi_3(\xi) = {} & e_1\left[\psi_3(\xi) - \psi_3(s) - \sum_{k_i}\frac{(G_H(k_i\xi) - G_H(k_is))}{F(k_i)}\bar{\psi}_3(k_i)\right]\\
& + e_2\int_s^\xi \frac{1}{\xi}\left[\psi_3(\xi) - \sum_{k_i}\frac{G_H(k_i\xi)}{F(k_i)}\bar{\psi}_3(k_i)\right]\mathrm{d}\xi,
\end{aligned}
\tag{41c}
$$

$$\Phi_4(\xi) = e_1\left[\psi_4(\xi) - \psi_4(s) - \sum_{k_i}\frac{(G_H(k_i\xi) - G_H(k_i s))}{F(k_i)}\bar{\psi}_4(k_i)\right] + e_2\int_s^\xi \frac{1}{\zeta}\left[\psi_4(\xi) - \sum_{k_i}\frac{G_H(k_i\xi)}{F(k_i)}\bar{\psi}_4(k_i)\right]\mathrm{d}\xi - \ln\left(\frac{\xi}{s}\right), \tag{41d}$$

$$\Phi_{5i}(\xi) = e_1\frac{(G_H(k_i\xi) - G_H(k_i s))}{F(k_i)} + e_2\int_s^\xi \frac{1}{\xi}\frac{G_H(k_i\xi)}{F(k_i)}\,\mathrm{d}\xi, \tag{41e}$$

$$F_i(\tau) = F_{1i}(\tau) + \bar{\psi}_4(k_i)\omega_i\int_0^\tau d(t)\sin[\omega_i(\tau - t)]\,\mathrm{d}t, \tag{41f}$$

$$F_{1i}(\tau) = \omega_i\int_0^\tau \bar{\psi}(k_i,\tau)\sin[\omega_i(\tau - t)]\mathrm{d}t + \bar{\psi}_2(k_i)\omega_i\int_0^\tau p_a(t)\sin[\omega_i(\tau - t)]\,\mathrm{d}t + \bar{\psi}_3(k_i)\omega_i\int_0^\tau p_b(t)\sin[\omega_i(\tau - t)]\mathrm{d}t + \bar{u}_0(k_i)\cos(\omega_i\tau) + \bar{v_0}(k_i)\frac{1}{\omega_i}\sin(\omega_i\tau). \tag{41g}$$

When $\xi = 1$ at the outer electric boundary of the piezoelectric hollow cylinder, Eq. (40) can be rewritten as

$$\phi_b(\tau) = \Phi_1(1,\tau) + \Phi_2(1)p_a(\tau) + \Phi_3(1)p_b(\tau) + \Phi_4(1)d(\tau) + \sum_i \Phi_{5i}(1)F_i(\tau) + \phi_a(\tau). \tag{42}$$

Substituting $\tau = 0$ into Eq. (42), yields

$$d(0) = \frac{\phi_b(0) - \phi_a(0) - \Phi_1(1,\tau) - \Phi_2(1)p_a(0) - \Phi_3(1)p_b(0) - \sum_i \Phi_{5i}(1)F_i(0)}{\Phi_4(1)}. \tag{43}$$

Substituting Eq. (41d) into Eq. (42), yields

$$\vartheta(\tau) = M_1 d(\tau) + \sum_i M_{2i}\int_0^\tau d(t)\sin[\omega_i(\tau - t)]\,\mathrm{d}t, \tag{44}$$

where

$$\vartheta(\tau) = \phi_b(\tau) - \phi_a(\tau) - \Phi_1(1,\tau) - \Phi_2(1)p_a(\tau) - \Phi_3(1)p_b(\tau) - \sum_i \Phi_{5i}(1)F_{1i}(\tau)M_1 = \Phi_4(1),$$
$$M_{2i} = \Phi_{5i}(1)\bar{\psi}_4(k_i)\omega_i. \tag{45}$$

It is seen that Eq. (44) is the Volterra integral equation of the second kind (Kress, 1989). In the following, Eq. (44) is solved by using the recursion formula based on linear interpolation function. In order to show the method of solving the integral Eq. (44), the time interval $[0,\tau]$ is firstly divided into n subintervals. The discrete time points are $\tau_0 = 0, \tau_1, \tau_2, \ldots, \tau_n$. Then the interpolation function at the time interval $[\tau_{j-1}, \tau_j]$ is expressed as

$$d(\tau) = \eta_j^0(\tau)d(\tau_{j-1}) + \eta_j^1(\tau)d(\tau_j) \quad (j = 1,2,\ldots,n), \tag{46}$$

where

$$\eta_j^0(\tau) = \frac{\tau - \tau_j}{\tau_{j-1} - \tau_j}, \quad \eta_j^1(\tau) = \frac{\tau - \tau_{j-1}}{\tau_j - \tau_{j-1}} \quad (j = 1,2,\ldots,n). \tag{47}$$

Substituting Eq. (46) into Eq. (44), gives

$$\vartheta(\tau_j) = M_1 d(\tau_j) + \sum_i M_{2i}\sum_{k=1}^{j}\left[R_{ijk}d(\tau_{k-1}) + S_{ijk}d(\tau_k)\right], \tag{48}$$

where

$$\begin{aligned} R_{ijk} &= \int_{\tau_{k-1}}^{\tau_k} \eta_k^0(t)\sin[\omega_i(\tau - t)]\,\mathrm{d}t \\ S_{ijk} &= \int_{\tau_{k-1}}^{\tau_k} \eta_k^1(t)\sin[\omega_i(\tau - t)]\,\mathrm{d}t \end{aligned} \quad (k = 1,2,\ldots,j,\ j = 1,2,\ldots,n). \tag{49}$$

From Eq. (48), yields

$$d(\tau_j) = \frac{\vartheta(\tau_j) - \sum_i M_{2i}\sum_{k=1}^{j-1}[R_{ijk}d(\tau_{k-1}) + S_{ijk}d(\tau_k)] - d(\tau_{j-1})\sum_i M_{2i}R_{ijj}}{M_1 + \sum_i M_{2i}S_{ijj}} \quad (j = 1,2,\ldots,n) \tag{50}$$

Substituting $d(0)$ in Eq. (43) into Eq. (48), $d(\tau_j)$ can be obtained, $(j = 1,2,\ldots,n)$ step by step, and determine $d(\tau)$. Substituting $d(\tau)$ obtained from Eq. (50) into Eq. (39), gives the exact expression of the solution, $u(\xi,\tau)$, for the basic equation of magneto–thermo–electro–elastic motion in the piezoelectric hollow cylinder. Thus, the corresponding transient stresses $\sigma_r(\xi,\tau), \sigma_\theta(\xi,\tau)$, the transient electric displacement $D_r(\xi,\tau)$, the transient electric potential $\phi(\xi,\tau)$ and perturbation of magnetic field vector $h_z(\xi,\tau)$ are easily obtained from Eqs. (9), (13) and (5b).

4. Numerical results and discussion

Transient responses and distributions of the piezoelectric hollow cylinder placed in an axial magnetic field, subjected to complex loadings are considered. A transitory temperature change produced by a sudden electric current pulse or by absorption of electromagnetic wave, is typically of a duration much less than 1 μs and may be expressed as

$$T(r,t) = T_0\left(1 - \frac{r-a}{2(b-a)}\right)H(t), \tag{51}$$

where T_0 is taken as 1, and $H(t)$ expresses the Heaviside function.

In the numerical calculations, material constants are selected for the piezoelectric hollow cylinder as follows:

$$\begin{aligned} &c_{11} = c_{33} = 111.0\ \text{GPa}, \quad c_{22} = 220.0\ \text{GPa}, \quad c_{13} = c_{23} = 115.0\ \text{GPa}, \quad e_{11} = 15.1\ (\text{V m N}^{-1}), \\ &e_{12} = e_{13} = -5.2\ (\text{V m N}^{-1}), \quad \alpha_1 = \alpha_3 = 0.0001\ (\text{K}^{-1}), \quad \alpha_2 = 0.00001\ (\text{K}^{-1}), \\ &g_{11} = 5.62\times 10^{-9}\ (\text{N V}^{-2}), \quad \beta_1 = -2.5\times 10^{-5}(\text{N V}^{-1}\ \text{m}^{-1}\ \text{K}^{-1}), \quad \rho = 4350\ (\text{kg m}^{-3}). \end{aligned}$$

The dynamic responses in the piezoelectric hollow cylinder subjected to a suddenly mechanical load on the internal surface are to be considered. The corresponding boundary conditions are expressed as

$$\sigma_r(1,\tau) = \sigma_0 H(\tau), \quad \sigma_r(1,\tau) = 0, \quad \phi_a(s,\tau) = 0, \quad \phi_b(1,\tau) = 0, \tag{52}$$

where σ_0 is a constant pressure, the non-dimensional $\sigma_i^* = \frac{\sigma_i}{\sigma_0}\ (i = r,\theta)$, $D_r^* = \frac{D_r}{\sigma_0}$, $\phi^* = \frac{\phi}{\sigma_0}$ and $h_z^* = \frac{h_z}{\sigma_0}$ are introduced in Figs. 1–10.

Example 1. The wall thickness ratio is $s = 1/21$, the dimensionless time is taken as $\tau 1 = \frac{C_L\tau}{sC_{v_0}} = \frac{C_L t}{a}$, and the dimensionless radial coordinate is taken as $R = \frac{\xi - s}{s} = \frac{r-a}{a}$. The response histories and distributions of the dynamic stresses for $R = 20$ are shown in Figs. 1 and 2. In order to avoid the effects of reflected waves, the computing time $\tau 1 = 20$ is taken. Figs. 1, 2 and 5, respectively, show the response histories of radial, hoop stresses and perturbation of magnetic field vector at different radial points. It is easy seen that the stresses responses and perturbation of magnetic field vector at some points is essentially zero before the arrival of the wavefront, and have strong discontinuities at the points where the wavefront arrives at. The amplitude of the wavefront decays gradually, and the dynamic response approaches to the quasi-static

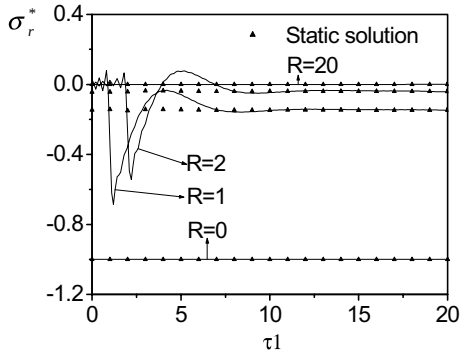

Fig. 1. Response histories of dynamic stress σ_r^* at $R = 0$, $R = 1$, $R = 2$, and $R = 20$ where $R = \frac{r-a}{a}$, $\tau 1 = \frac{C_L t}{a}$.

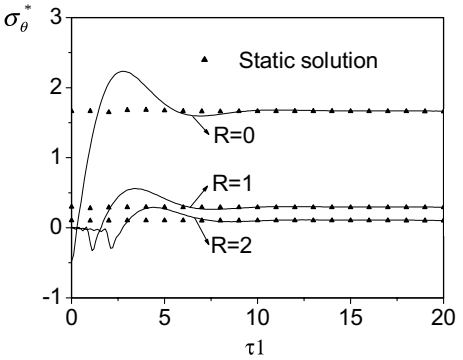

Fig. 2. Response histories of dynamic stress σ_θ^* at $R = 0$, $R = 1$, and $R = 2$, where $R = \frac{r-a}{a}$, $\tau 1 = \frac{C_L t}{a}$.

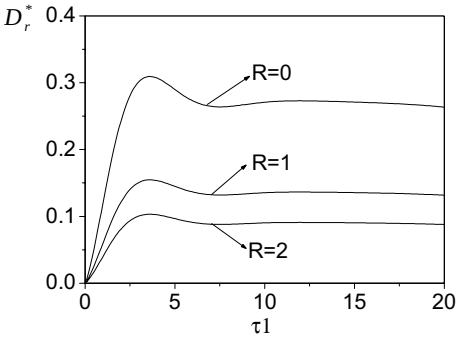

Fig. 3. Response histories of dynamic electric displacement D_r^*, at $R = 0$, $R = 1$ and $R = 2$, where $R = \frac{r-a}{a}$, $\tau 1 = \frac{C_L t}{a}$.

solution at the same point when time is large and the effect of reflected does not appear. Figs. 3 and 4 illustrate the response histories and distributions of the electric displacement $D_r(\xi, \tau)$ and the electric potential $\phi(\xi, \tau)$ at the different radial points in the piezoelectric hollow cylinder subjected to a suddenly

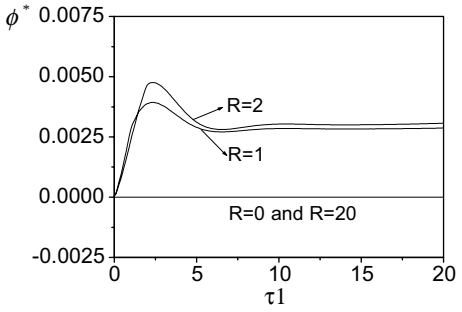

Fig. 4. Response histories of dynamic electric potential ϕ*, at $R = 0$, $R = 1$, $R = 2$ and $R = 20$, where $R = \frac{r-a}{a}$, $\tau 1 = \frac{C_L t}{a}$.

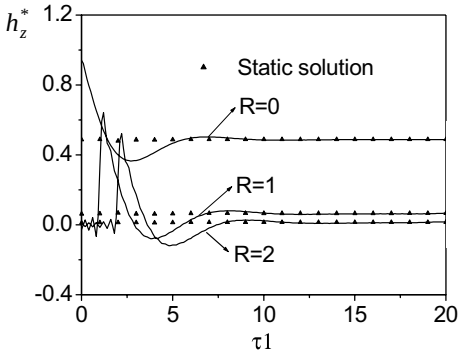

Fig. 5. Response history of perturbation of magnetic field vector h_z^* at $R = 0$, $R = 1$ and $R = 2$, where $R = \frac{r-a}{a}$, $\tau 1 = \frac{C_L t}{a}$.

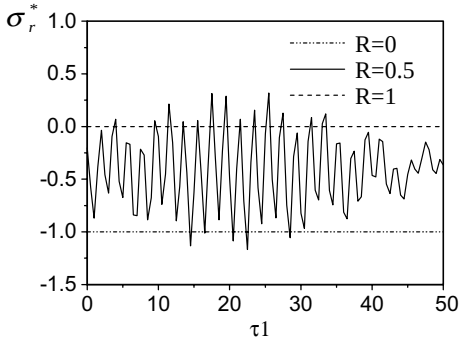

Fig. 6. Response histories of the transient radial stresses σ_r^* at $R = 0$, $R = 0.5$, and $R = 1$, where $R = \frac{r-a}{b-a}$, $\tau 1 = \frac{C_L t}{b-a}$, $\sigma_r^* = \frac{\sigma_r}{\sigma_0}$.

pressure on the internal surface. From Figs. 3 and 4, it is easy seen that the response histories and distributions of the electric displacements $D_r(\xi, \tau)$and the electric potential $\phi(\xi, \tau)$ are similar to that of the dynamic stresses. They will also arrive finally at a steady value when time τ is large and the effect of reflected does not appear. From Fig. 4, it is seen that the electric potential $\phi(\xi, \tau)$ at the internal and external boundary equal zero, which satisfy the prescribed electric boundary conditions. The above

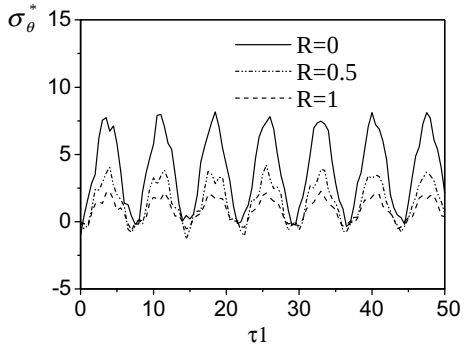

Fig. 7. Response histories of the transient hoop stress σ_θ^* at $R = 0$, $R = 0.5$, and $R = 1$, where $R = \frac{r-a}{b-a}$, $\tau 1 = \frac{C_L t}{b-a}$, $\sigma_\theta^* = \frac{\sigma_\theta}{\sigma_0}$.

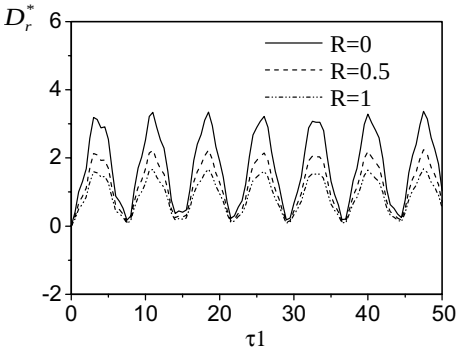

Fig. 8. Response histories of the transient electric displacements D_r^*, at $R = 0$, $R = 0.5$, and $R = 1$, where $R = \frac{r-a}{b-a}$, $\tau 1 = \frac{C_L t}{b-a}$, $D_r^* = \frac{D_r}{\sigma_0}$.

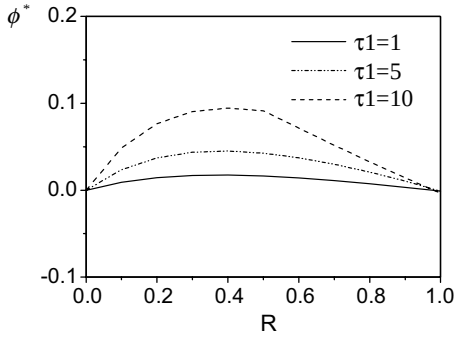

Fig. 9. Distributions of the transient electric potentials ϕ^*, at $\tau 1 = 1$, $\tau 1 = 5$ and $\tau 1 = 10$, where $R = \frac{r-a}{b-a}$, $\tau 1 = \frac{C_L t}{b-a}$, $\phi^* = \frac{\phi}{\sigma_0}$.

described shows that the solution in the paper possesses wave properties, and the correction of the numerical results is clarified.

In the following two examples, the internal radius of the piezoelectric hollow cylinder is taken as $a = 0.01$ m, and the wall thickness ratio is taken as $s = 1/2$. The dimensionless time is taken as

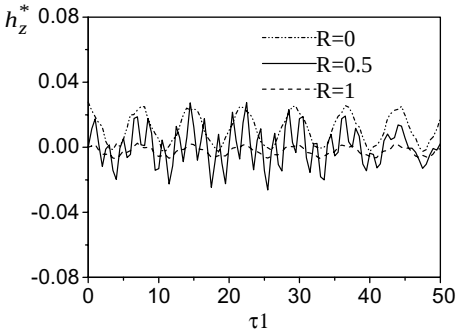

Fig. 10. Response histories of perturbation of magnetic field vector h_z^*, at $R = 0$, $R = 0.5$ and $R = 1$ where $R = \frac{r-a}{b-a}$, $\tau 1 = \frac{C_L t}{b-a}$, $h_z^* = \frac{h_z}{\sigma_0}$.

$\tau 1 = \frac{C_L \tau}{(1-s)C_v} = \frac{C_L t}{b-a}$, the dimensionless radial coordinate, $R = \frac{\xi - s}{1-s} = \frac{r-a}{b-a}$ and the response time is taken as $\tau 1 = 50$.

Example 2. Other conditions are the same as Example 1. Figs. 6 and 7, respectively, show the response histories of radial and hoop stresses at different radial points. Because of the small wall thickness, the effects of wave reflected between the inner-wall and outer-wall appear. From Fig. 6, it is shown that except the radial stresses at the internal and external surfaces of the piezoelectric hollow cylinder satisfy the given zero boundary condition, and the stresses at other points oscillate dramatically because of the effect of wave reflected between the inner wall and outer wall. From Figs. 7 and 8, it is seen that the peak values of hoop stresses and electric displacements decrease gradually from internal wall to external wall at the identical time τ. It is seen in Fig. 9 that the electric potential ϕ^* at the internal and external boundaries equal zero, which satisfy the prescribed electric boundary conditions (52), and the distribution of the electric potential ϕ^* along radius is non-linear at different non-dimensional time τ. Fig. 10 depicts the response histories of magnetic field vector at different radial points. It is seen easily from the curve that the magnitude value of perturbation of magnetic field vector becomes small from the internal wall to external wall of the piezoelectric hollow cylinder.

Example 3. Consider that the transient responses of the piezoelectric hollow cylinder subjected to thermal shock load $T(r,t)$ in Eq. (51), and electric excitation induced by inhomogeneous electric boundary conditions (53). The inhomogeneous electric boundary condition are written as

$$\sigma_r(1,\tau) = 0, \quad \sigma_r(1,\tau) = 0, \quad \phi_a(s,\tau) = 0, \quad \phi_b(1,\tau) = \phi_0 H(\tau), \tag{53}$$

where ϕ_0 is a constant electric potential, the non-dimensional $\sigma_i^* = \frac{\sigma_i}{\phi_0}(i = r, \theta)$, $D_r^* = \frac{D_r}{\phi_0}$, $\phi^* = \frac{\phi}{\phi_0}$ and $h_z^* = \frac{h_z}{\phi_0}$ are introduced in Figs. 11–15.

From Figs. 11 and 14, it is seen that the radial stresses and the electric potential at the boundaries $R = 0, 1$ satisfy the given boundary conditions. Except the points at given boundary condition, transient responses at other points oscillates dramatically as shown in Figs. 11 and 14. It is seen from Fig. 11 that the maximum amplitude of radial compression stress is larger than that of radial tension stress. Fig. 12 shows that the amplitude of hoop compression stress at the internal wall of the piezoelectric hollow cylinder is larger than the amplitude of hoop tension stress. However, the amplitude of hoop compression stress at the external wall of the piezoelectric hollow cylinder is less than the amplitude of hoop tension stress, which is shown in Fig. 12. The response histories of electric displacement always are negative as shown in Fig. 13. This is similar change as shown in Fig. 8. It is seen in Fig. 14 that the distribution of the electric potential ϕ^* along radius is weak non-linear at different non-dimensional time τ. Comparing Figs. 15 and 10, it is seen

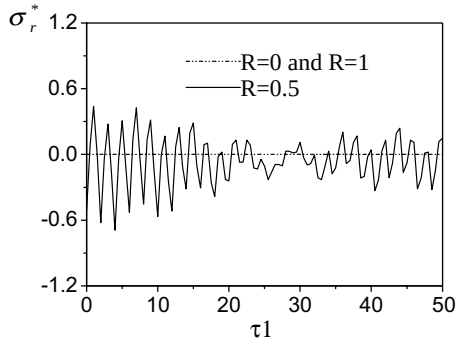

Fig. 11. Response histories of the transient radial stresses σ_r^* at $R = 0$, $R = 0.5$ and $R = 1$, where $R = \frac{r-a}{b-a}$, $\tau 1 = \frac{C_L t}{b-a}$, $\sigma_r^* = \frac{\sigma_r}{\phi_0}$.

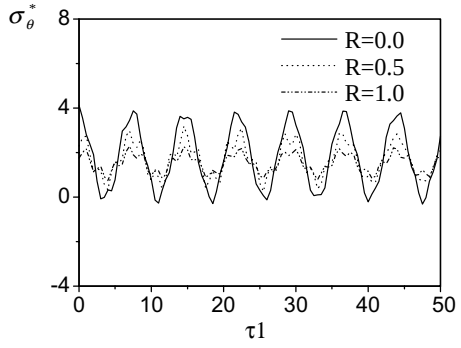

Fig. 12. Response histories of the transient hoop stresses σ_θ^* at $R = 0$, $R = 0.5$, and $R = 1$, where $R = \frac{r-a}{b-a}$, $\tau 1 = \frac{C_L t}{b-a}$, $\sigma_\theta^* = \frac{\sigma_\theta}{\phi_0}$.

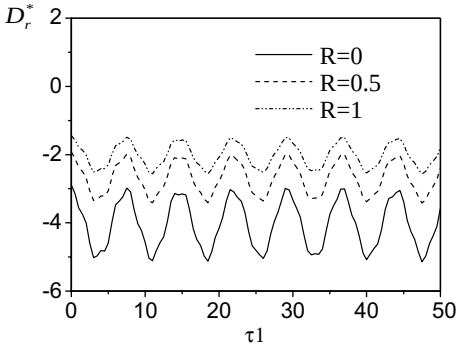

Fig. 13. Response histories of the transient electric displacements D_r^*, at $R = 0$, $R = 0.5$ and $R = 1$, where $R = \frac{r-a}{b-a}$, $\tau 1 = \frac{C_L t}{b-a}$, $D_r^* = \frac{D_r}{\phi_0}$.

that the histories and distribution of perturbation of magnetic field vector caused by the sudden unit electric potential is similar to that caused by the sudden unit pressure, but the responded amplitude of perturbation of magnetic field vector caused by the sudden unit electric potential is larger than that caused by the sudden unit pressure.

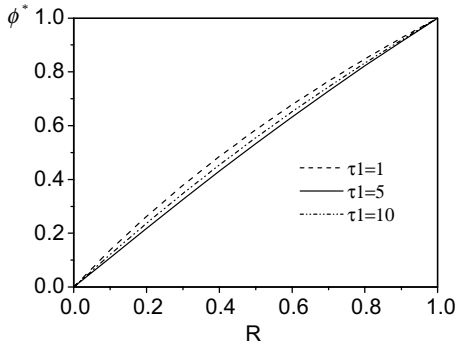

Fig. 14. Distributions of the transient electric potentials ϕ*, at $\tau 1 = 1$, $\tau 1 = 5$ and $\tau 1 = 10$, where $R = \frac{r-a}{b-a}$, $\tau 1 = \frac{C_L t}{b-a}$, $\phi^* = \frac{\phi}{\phi_0}$.

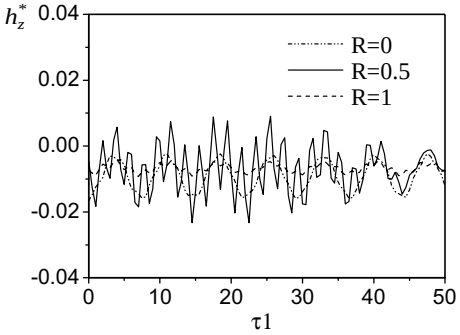

Fig. 15. Response histories of perturbation of magnetic field vector h_z^*, at $R = 0$, $R = 0.5$ and $R = 1$ where $R = \frac{r-a}{b-a}$, $\tau 1 = \frac{C_L t}{b-a}$, $h_z^* = \frac{h}{\phi_0}$.

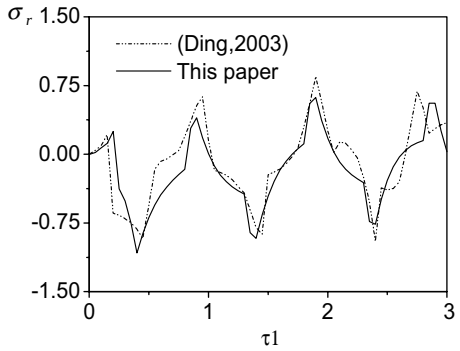

Fig. 16. Response histories of radial stress σ_r, at $R = 0.5$ in the piezoelectric hollow cylinder no considering an axial magnetic field load and thermal shock, where $R = \frac{r-a}{b-a}$, $\tau 1 = \frac{C_L t}{b-a}$.

Example 4. In order to prove further the correctness of analytical results in the paper, omitting the axial magnetic field load and thermal shock, the present method can be applied to solve the transient problem of piezoelectric hollow cylinders. For ease of comparison with reference (Ding et al., 2003), the same transient problem of the piezoelectric hollow cylinder no considering an axial magnetic field load and thermal shock

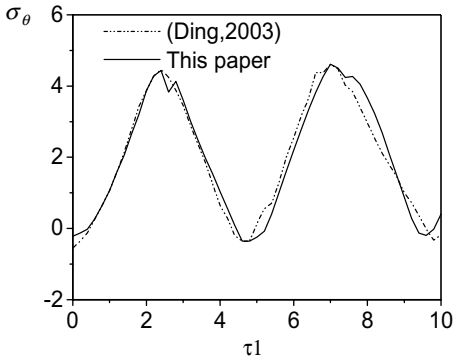

Fig. 17. Response histories of hoop stress σ_θ, at $R = 0$, in the piezoelectric hollow cylinder no considering an axial magnetic field load and thermal shock, where $R = \frac{r-a}{b-a}$, $\tau 1 = \frac{C_L t}{b-a}$.

is taken and the same parameters are taken: the ratio of internal radius to external radius $s = a/b = 1/2$, the dimensionless radial coordinate $R = \frac{r-a}{b-a}$ and dimensionless time $\tau 1 = \frac{C_L t}{b-a}$. The boundary conditions are expressed in Eq. (52). From Figs. 16 and 17, one can see that the results from the two different methods are nearly the same.

5. Conclusions

1. Comparing Example 2 with Example 3, it is seen that the response histories and distributions of stresses, electric displacement, electric potential and perturbation of magnetic field in a piezoelectric hollow cylinder are obviously different for two kinds of boundary conditions which are, respectively, shown in Eqs. (52) and (53). Thus, it is possible to control the response histories and distribution of magneto–thermo–electro–elastic stresses in the piezoelectric hollow cylinder by applying a suitable thermal load, mechanical load and electric excitation load to the structure, or to assessment the response histories and distributions of magneto–thermo–electro–elastic stresses in the piezoelectric hollow cylinder by measuring the response histories of electric potential in the structure.
2. It is noted that while solving the present problem, the number of eigenvalue terms was taken to be only 40, and the relative error in the results obtained was less 1%, from this knowledge of the response histories for magneto–thermo–electro–elastic stresses, electric displacement, electric potential and perturbations of an axial magnetic field in the piezoelectric hollow cylinder. We can design various electromagnetoelastic elements under complex loads to meet special engineering requirements.
3. It is concluded from the above analyses and results that the present solution is accurate and reliable, and the method is simple and effective. So it may be used as a reference to solve other transient problems of coupled magneto–thermo–electro–elasticity.

References

Chandrasekharaiah, D.S.A., 1988. Generalized linear thermoelasticity theory for piezoelectric media. Acta Mechanica 71, 39–49.
Cinelli, G., 1965. An extension of the finite Hankel transform and application. International Journal of Engineering Science 3, 539–559.

Dai, H.L., Wang, X., 2004. Dynamic responses of piezoelectric hollow cylinders in an axial magnetic field. International Journal of Solids and Structures 41, 5231–5246.

Ding, H.J., Chen, W.Q., Guo, Y.M., Yang, Q.D., 1997. Free vibration of piezoelectric cylindrical shells filled with compressible fluid. International Journal of Solids and Structures 34, 2025–2034.

Ding, H.J., Wang, H.M., Hou, P.F., 2003. The transient responses of piezoelectric hollow cylinders for axisymmetric plane strain problems. International Journal of Solids and Structures 40, 105–123.

Kapuria, S., Dumir, P.C., Sengupta, S., 1996. Exact piezothermoelastic axisymmetric solution of a finite transversely isotropic cylindrical shell. Computer and Structures 61 (6), 1085–1099.

Kapuria, S., Sengupta, S., Dumir, P.C., 1997. Three-dimensional solution for a hybrid cylindrical shell under axisymmetric thermoelectric load. Archive of Applied Mechanics 67 (5), 320–330.

Kraus, J.D., 1984. Electromagnetics. McGrawHill, Inc., USA.

Kress, R., 1989. Linear Integral EquationApplied Mathematical Sciences, 82. Springer-Verlag World Publishing Corp.

Lekhniskii, S.G., 1981. Theory of Elasticity of an Anisotropic Body. Mir Publishers, Moscow.

Mithchell, J.A., Reddy, J.N., 1995. A study of embedded piezoelectric layers in composite cylinders. Journal of Applied Mechanics 62, 166–173.

Raja, S., Rohwer, K., Rose, M., 1999. Piezothermoelastic modeling and active vibration control of laminated composite beams. Journal of Intelligent Material Systems and Structures 10 (11), 890–899.

Rao, S.S., Sunar, M., 1993. Analysis of distributed thermopiezoelectric sensors and actuators in advanced intelligent structures. AIAA Journal 31, 1280–1286.

Rao, S.S., Sunar, M., 1994. Piezoelectricity and its use in disturbance sensing and control of flexible structures. Applied Mechanics Reviews 47 (4), 113–123.

Ray, M.C., Rao, K.M., Samanta, B., 1992. Exact analysis of coupled electroelastic behavior of piezoelectric plate under cylindrical bending. Computer and Structures 45, 667–677.

Ray, M.C., Rao, K.M., Samanta, B., 1993. Exact analysis for static analysis of an intelligent structure under cylindrical bending. Computer and Structures 47, 1031–1042.

Shul'ga, N.A., Grigorenko, A.Y., Loza, I.A., 1984. Axisymmetric electroelastic waves in a hollow piezoelectric ceramic cylinder. Prikladnaya Mekhanika 20 (1), 26–32.

Tauchert, T.R., 1992. Piezothermoelastic behavior of a laminated plate. Journal of Thermal Stresses 15, 25–37.

Wang, X., Lu, G., 2002. Magnetothermodynamic stress and perturbation of magnetic field vector in a solid cylinder. Journal of Thermal Stresses 25, 909–926.